On the Sequential Hydrogen Dissociative Chemisorption on Small Platinum Clusters: A Density Functional Theory Study

ARTICLE *in* THE JOURNAL OF PHYSICAL CHEMISTRY C · AUGUST 2007

Impact Factor: 4.77 · DOI: 10.1021/jp073597e · Source: OAI

6 AUTHORS, INCLUDING:

Chenggang Zhou
China University of Geosciences
46 PUBLICATIONS **505** CITATIONS
SEE PROFILE

Robert Forrey
Pennsylvania State University
137 PUBLICATIONS **1,760** CITATIONS
SEE PROFILE

Hansong Cheng
China University of Geosciences
166 PUBLICATIONS **2,385** CITATIONS
SEE PROFILE

On the Sequential Hydrogen Dissociative Chemisorption on Small Platinum Clusters: A Density Functional Theory Study

Chenggang Zhou,[†] Jinping Wu,[†] Aihua Nie,[†] Robert C. Forrey,[‡] Akitomo Tachibana,[§] and Hansong Cheng*,[||]

Institute of Theoretical Chemistry and Computational Materials Science, China University of Geosciences, Wuhan 430074, China, Department of Physics, Penn State University, Berks Campus, Reading, Pennsylvania 19610-6009, Department of Microengineering, Kyoto University, Kyoto 606-8501, Japan, and Air Products and Chemicals, Incorporated, 7201 Hamilton Boulevard, Allentown, Pennsylvania 18195-1501

Received: May 10, 2007; In Final Form: June 25, 2007

We present a simple cluster model to understand the dissociative chemisorption of molecular hydrogen and the desorption of atomic hydrogen on platinum small clusters using the gradient-corrected density functional theory. Successive H_2 decomposition and sequential H desorption on the selected Pt_n ($n = 2-5, 7-9$) clusters were systematically studied, and the H_2 dissociative chemisorption energies and the H desorption energies at the full H saturation were identified. The reaction processes are driven by charge transfer from Pt atoms to H atoms assisted by strong orbital overlaps between Pt 5d orbitals and H 1s orbital, which leads to electron delocalization in large clusters of metal hydrides. It was found that the number of H atoms chemisorbed on the small Pt clusters increases almost linearly with the size of the selected Pt cluster.

1. Introduction

Molecular hydrogenation is one of the most important chemical reactions, widely used in petrochemical, pharmaceutical, and fine chemical production. Many of the reactions are catalyzed by precious metals such as platinum and palladium.[1−3] Hydrogen molecules undergo a dissociative chemisorption process on these catalysts, which then supply hydrogen atoms to the unsaturated chemical bonds of gas species. A great deal of effort has been made in the past few decades to understand the underlying mechanisms of the catalytic processes in order to develop efficient, low-cost novel catalysts for hydrogenation.[4−6] Several studies using thermal desorption spectroscopy reported that the dissociative chemisorption energy of hydrogen on the Pt(111) surface is between 0.70 and 0.83 eV.[7−11] A recent desorption experiment of hydrogen/deuterium on a Pt_{13} cluster supported by NaY zeolite yielded an H_2 dissociative chemisorption energy of 1.36 eV.[12] Theoretically, the reported dissociative chemisorption energy of hydrogen on Pt crystalline surfaces ranges from 0.8 to 1.54 eV.[13−16] In contrast, the dissociative chemisorption of hydrogen calculated by Balasubramanian and co-workers[17,18] using multiconfiguration self-consistent field theory (MCSCF) on Pt_2 and Pt_3 clusters is 0.93−1.33 eV. More recently, Okamoto[19] reported a chemisorption energy of 1.4 eV using a density functional theory/generalized gradient approximation (DFT/GGA) method for H_2 dissociatively adsorbed at the on-top sites of a Pt_{13} cluster, which is in agreement with experimental results.[12] These results clearly demonstrate that the chemical reactivity of H_2 on clusters is much higher than on crystalline surfaces. Furthermore, several calculations also suggested substantially high desorption energy for atomic hydrogen adsorbed on catalyst surfaces.[20] The desorption energy of a H atom on the Pt(111) surface was reported to be 2.60−2.65 eV,[21−23] while the local density functional theory calculations by Watari and Ohnishi[24] on H desorption on a Pt_{13} cluster gave a desorption energy of 2.9−4.5 eV. Clearly, for both the H_2 dissociative chemisorption and H desorption processes, clusters exhibit considerably higher reactivity toward hydrogen than crystalline surfaces, which is largely due to the finite size effect since clusters exhibit more sharp corners and edges.

Very recently, Cheng and co-workers[25] reported strong coverage dependency of chemical reactivity of a Pt_6 cluster toward hydrogen. It was found that, upon H saturation on the cluster, the calculated dissociative chemisorption energy is only slightly higher than the value on the Pt(111) surface, while the H desorption energy is slightly lower than what was reported on the surface. Clusters with full coverage of gas species can serve as a more realistic model for catalysts under typical catalytic conditions in which a constant pressure of gas species is always maintained and thus the surfaces of the catalysts in general are fully covered. In this paper, we present results on H_2 dissociative chemisorption and H desorption on other small Pt_n ($n = 2-5, 7-9$) clusters using DFT under generalized gradient approximation (GGA). We first performed systematic calculations on sequential H_2 dissociative chemisorption on these clusters until they are fully saturated by H atoms. The main purpose of the present study is to understand the cluster size-dependency of H_2 dissociative chemisorption and H desorption energies at full saturation. It is expected that a definitive conclusion on this subject would provide useful information on the catalytic activities of various sizes of clusters and thus facilitate catalyst design and development. The structures of small Pt clusters have been extensively studied previously.[26,27] Very recently, we have identified some of the energetically most stable structures of small Pt clusters.[28] Therefore, in the present study, we will concentrate only on these clusters and explore their reactivity toward hydrogen.

[†] China University of Geosciences.
[‡] Penn State University.
[§] Kyoto University.
[||] Air Products and Chemicals, Inc.

10.1021/jp073597e CCC: $37.00
Published on Web 08/07/2007

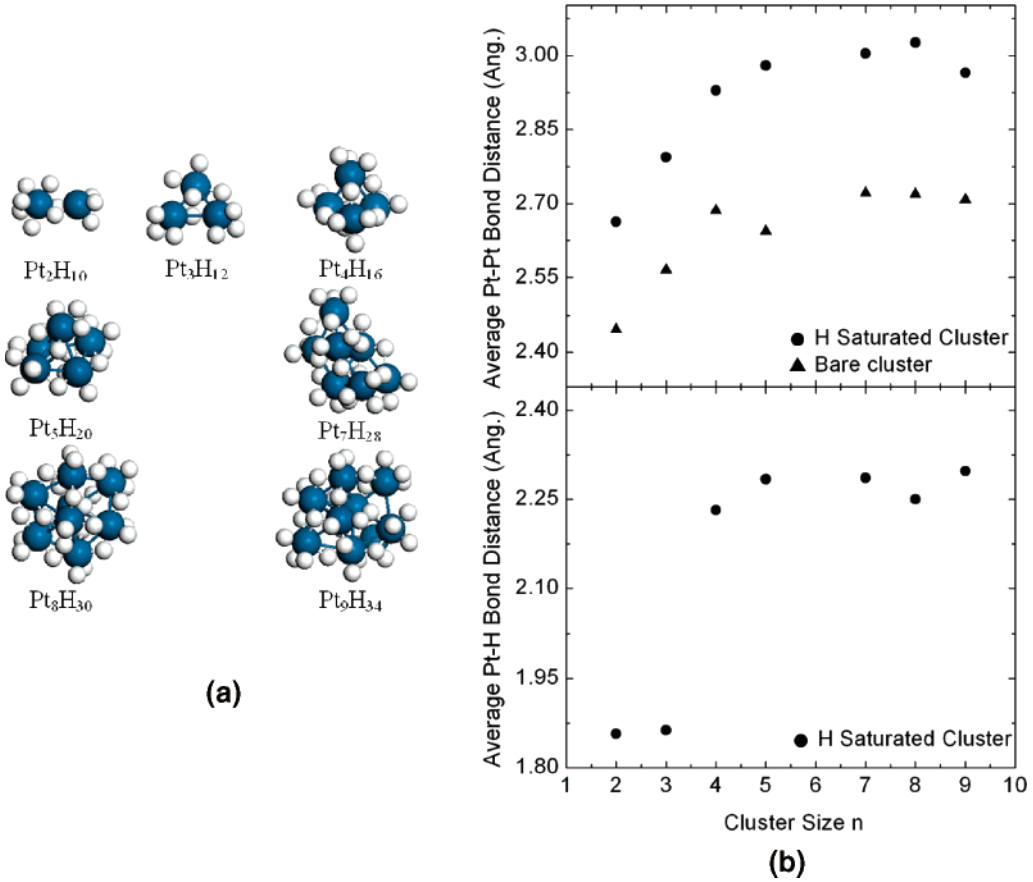

Figure 1. (a) Optimized Pt_nH_m clusters and (b) average Pt−Pt and Pt−H distances at full H saturation.

2. Computational Method

All calculations are performed via DFT/GGA with the nonlocal exchange−correlation functional proposed by Perdew and Wang (PW91).[29,30] The method was implemented in the Dmol[3] package.[31−33] Double precision numerical basis sets augmented with polarization functions (DNP) were use to describe the valence electrons, while the effective core pseudopotential (ECP) were utilized to describe the core electrons, which account for the relativistic effect important for Pt atoms. A spin-polarized scheme was employed to deal with the electronically open-shell systems intrinsic to the Pt atoms. The Hirshfeld population analysis was performed to analyze the charge transfer.[34] The Mulliken population analysis is inappropriate due to its indiscriminative division scheme in the present case since the size of the Pt atom is much larger than that of H. All structures are fully optimized without symmetry constraints to obtain energetically most stable structures by use of the conjugated gradient algorithm. The transition state (TS) structure search was performed only for Pt_2 to gain insight into the barrier of H_2 dissociative chemisorption by the LST/QST method.[35] TS structures were verified by performing normal-mode analysis that gives only one imaginary frequency. Subsequently, the average chemisorption energy per molecule was evaluated by use of the equation:

$$\Delta E_{CE} = 2\,(E_{Ptn} + m/2E_{H2} - E_{PtnHm})/m \quad (n = 2, 3, ...; m = 2, 4, 6, ...) \quad (1)$$

where E_{Ptn} represents the energy of the Pt_n cluster, E_{H2} is the energy of H_2 molecule, and E_{PtnHm} is the total energy of m hydrogen atoms adsorbed on Pt_n cluster.

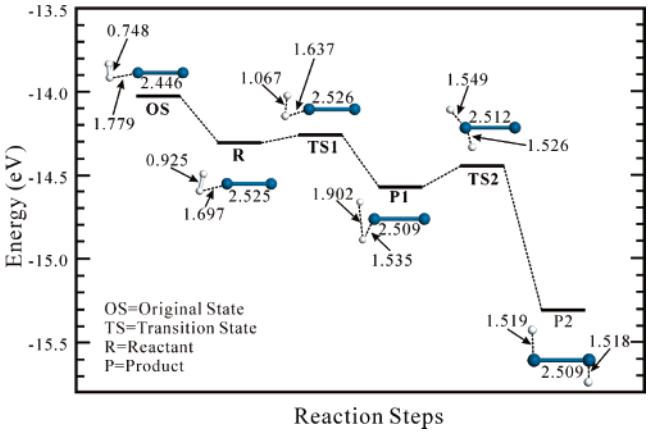

Figure 2. Reaction pathway of H_2 activated by Pt_2 cluster. The unit for the bond length/distance is angstroms. The reaction barrier is 0.05 eV from reactant to product1 and 0.13 eV from product1 to product2.

One of the central issues in catalytic hydrogenation is how readily the chemisorbed H atoms desorb from the catalyst. To address this issue, it is important to identify the H desorption energy at or near full saturation of the catalyst. Accordingly, we calculated the sequential desorption energy per atom using the equation defined in ref 25:

$$\Delta E_{DE} = E_H - (E_{PtnHm} - E_{PtnHm-2})/2 \quad (n = 2, 3, ...; m = 2, 4, 6, ...) \quad (2)$$

where E_H is the energy of H atom. At full saturation, the sequential desorption energy ΔE_{DE} represents the threshold energy required for a H atom to desorb from the cluster surface.

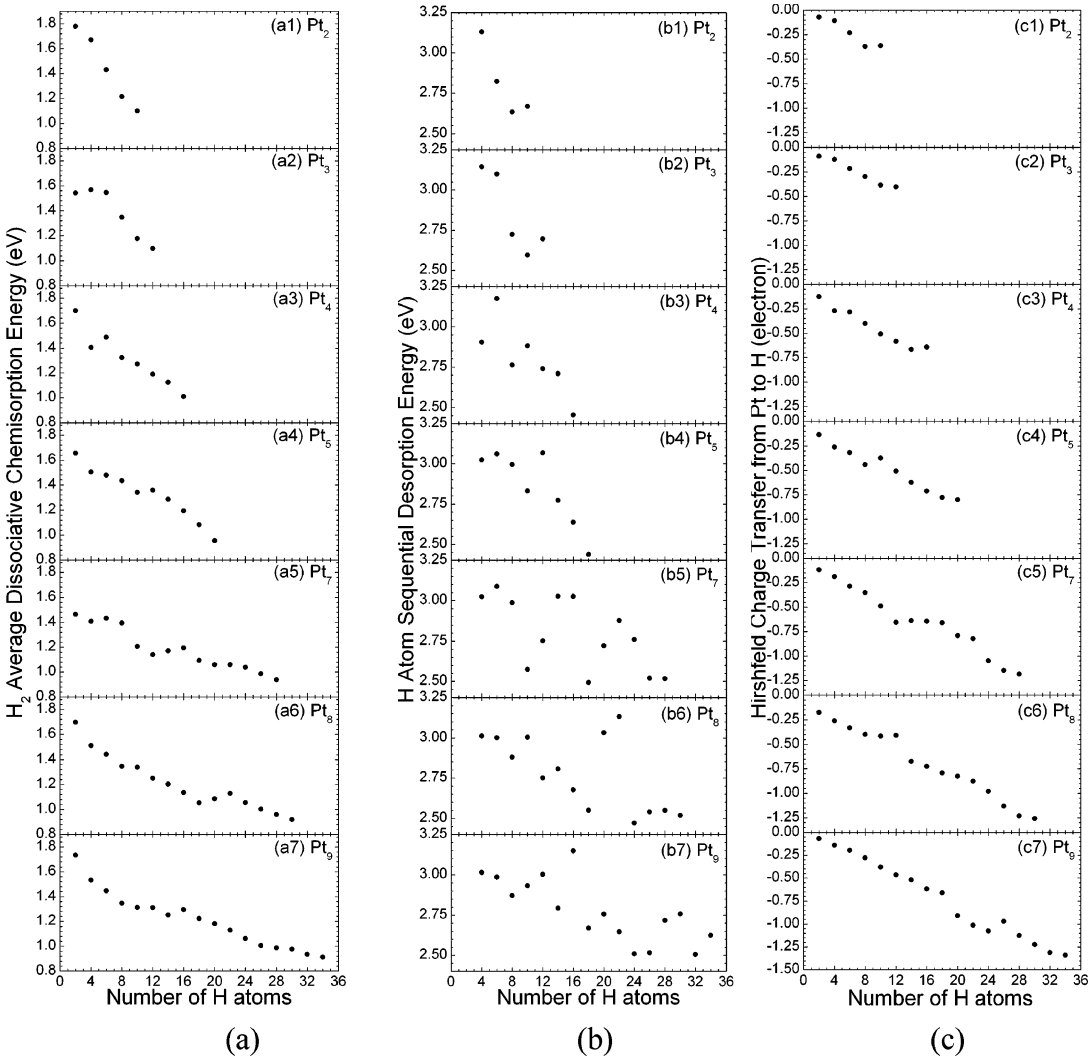

Figure 3. (a) Calculated H_2 dissociative chemisorption energy, (b) H desorption energy, and (c) loss of Hirshfeld charges of Pt clusters vs H coverage.

To quantify whether the Pt cluster is fully saturated or not, we performed ab initio molecular dynamics (MD) simulation at room temperature for 2 ps with a time step of 1 fs in a NVT canonical ensemble using the Nosé-Hoover chain[36,37] for temperature control to ensure all H atoms remain chemisorbed. Excessive H atoms on the surface will recombine into H_2 molecules physisorbed on the cluster upon the MD runs.

3. Results and Discussion

For the convenience of presentation, we will not describe all the optimized structures obtained. Instead, we will use Pt_2 to serve as an example for TS calculations for dissociative chemisorption of H_2 and Pt_4 tetrahedral structure to show the sequential H_2 dissociative chemisorption and H desorption. The fully optimized structures of the saturated clusters are shown in Figure 1a. All H atoms remain on the cluster surfaces. There are three possible adsorption sites on the Pt clusters: 1-fold on-top, 2-fold edge, and 3-fold hollow sites, each of which was examined for H adsorption strength. We first identified that the on-top site is energetically the most favorable for H_2 dissociation, followed by edge sites and hollow sites, in agreement with the previous DFT study.[25] We then sequentially increased the H loading on these clusters until they were fully saturated. To describe the structural characteristics, we show the calculated average bond distances of Pt−Pt and Pt−H vs cluster size in Figure 1b. For the average bond distances of Pt−Pt, we also compare with those of bare clusters. For bare clusters, the average Pt−Pt bond distance increases with the cluster size until $n = 4$; it levels out due to the structural transition from 2-D to 3-D, in which case each Pt atom is bonded with three or four Pt atoms. Upon H chemisorption, however, the average Pt−Pt bond distance is relaxed considerably by about 0.2−0.3 Å. In parallel, the average Pt−H bond distance increases substantially from $n = 3$ to $n = 4$, indicating weaker Pt−H bonds. Again, the effect of the structural transition is readily visible. The main reason is that each of the Pt atoms of the 3-D clusters participates in metallic bonding with more Pt atoms, which reduces the bond strength with H atoms.

There are numerous pathways that lead to the dissociative chemisorption of H_2 on the Pt_2 dimer, one of which was found to undergo two steps as shown schematically in Figure 2. The H_2 molecule approaches the dimer from one end of the dimer axis with the Pt atom vertically toward the center of mass of H_2, initially forming a weakly bonded species (R), which then undergoes a transition state (TS1) that leads to decomposition of H_2 with a barrier of 0.05 eV. The nearly barrierless dissociative chemisorption results in a T-shaped adsorption structure (P1), which lies 0.26 eV below the reactant state. The adsorbed H atom is capable of moving from one side of the dimer to the other (P2), with an energy barrier of 0.13 eV (TS2).

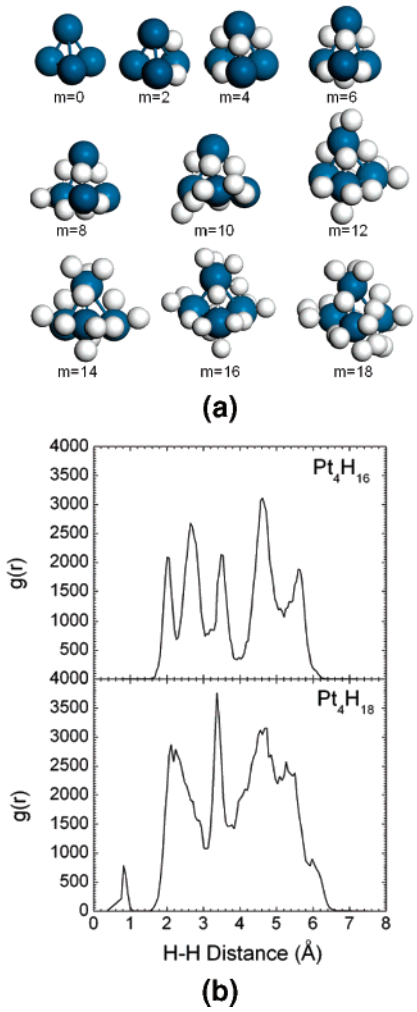

Figure 4. (a) Fully optimized structures of H_2 sequential dissociative chemisorption on a Pt_4 cluster. (b)Ccalculated H−H distance distribution function $g(r)$ for Pt_4H_{16} and Pt_4H_{18}, respectively. $g(r)$ was obtained by tabulating all the H−H distances at each step of the MD trajectories fit with Gaussian functions.

The calculation suggests that the H_2 dissociative chemisorption requires very little activation energy compared to the activation barrier of 0.06−0.42 eV for crystalline surface reported by Vincent et al.[14] Overall, the calculated chemisorption energy is 1.78 eV. The strong chemisorption arises from the orbital overlaps between the 1s orbital of H atoms and the 5d orbitals of Pt atoms, resulting in charge transfer from Pt 5d to H 1s. The calculated sequential H_2 chemisorption energy and sequential H desorption energy are shown in Figure 3, panels a1 and b1, respectively. The cluster was found to be able to accommodate up to 10 H atoms, beyond which additional H will recombine into H_2 molecules. Both ΔE_{CE} and ΔE_{DE} decrease as the number of H atoms on the cluster increases. Upon saturation, the calculated chemisorption energy is 1.1 eV, about 0.3−0.4 eV higher than the experimental value for H_2 on the Pt(111) surface.[7−11] In particular, it is interesting to note that the value of H_2 dissociation energy ΔE_{CE} drops substantially from 1.78 eV at a low coverage to 1.1 eV at full saturation, while the threshold H-desorption energy ΔE_{DE} at full coverage is about 0.6 eV lower than its value at a low coverage. The amount of Hirshfeld charge transferred from Pt_2 to the H atoms (ΔQ) is shown in Figure 3, panel c1, which declines with the number of H atoms and is consistent with the calculated ΔE_{CE}. For the Pt_3 trimer, the calculated ΔE_{CE}, ΔE_{DE}, and ΔQ exhibit almost the same trends as for the Pt_2 dimer. The cluster can

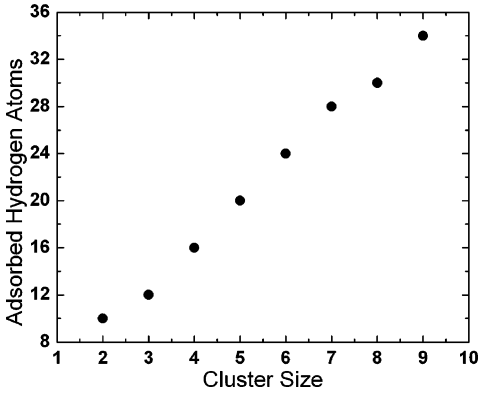

Figure 5. Number of H atoms on a cluster vs cluster size.

accommodate up to 12 H atoms. Substantial structural expansion as well as distortion of the triangular geometry of the cluster is observed upon hydrogen uptake.

To show the sequential adsorption of H, Figure 4a displays the fully optimized structures of Pt_4 clusters with various H coverages. The bare Pt_4 cluster adopts a tetrahedral configuration. Depending on the coverage, the cluster is distorted to a certain extent. Full saturation is realized at $m = 16$, where m is the number of H atoms. Excessive H adsorption would result in recombination of H atoms to form H_2 molecules. In fact, upon loading 18 H atoms on the cluster, we performed ab initio MD simulations for up to 2 ps. It was observed from the MD trajectories that two H atoms are readily squeezed out from the cluster, forming a H_2 molecule that is subsequently bonded to the cluster via weak interaction force. Indeed, the calculated H−H bond distance distribution for Pt_4H_{16} and Pt_4H_{18}, shown in Figure 4b, clearly illustrates that the smallest H−H distance for Pt_4H_{16} is around 2.1 Å, while for Pt_4H_{18} a peak around 0.75 Å indicates a H_2 molecule is formed. Once again, more charge flows from the Pt_4 cluster to H atoms as the H coverage increases (Figure 3, panel c2).

For larger Pt_n ($n > 4$) clusters, the calculated H_2 dissociative chemisorption energy ΔE_{CE}, H sequential desorption energy ΔE_{DE}, and loss of electrons of metal clusters ΔQ exhibit similar features to what were found for smaller clusters (Figure 3). The general trends of these quantities is that they decline with the H coverage. However, while both ΔE_{CE} and ΔQ decreases monotonically with the number of H atoms, some fluctuation of ΔE_{DE} is observed. This is because H atoms first saturate the energetically most favorable sites. As these sites become filled, their stability decreases and the vacant sites begin to fill. The fluctuation of ΔE_{DE} is due to the difference in chemisorption energies near the saturation boundary. Full H saturation can be ensured upon MD simulations, which eliminate H_2 molecules physisorbed on the clusters. Figure 3 indicates that in all cases, at the full saturation, the H_2 dissociative chemisorption energy fluctuates in the range between 0.9 and 1.1 eV, slightly higher than the experimental value for the H_2 dissociative chemisorption on the Pt(111) surface at zero coverage by 0.2−0.3 eV.[7−11] Similarly, the calculated threshold H sequential desorption energy varies in a narrow range of 2.45−2.60 eV, slightly smaller than the value for an isolated H atom on the Pt(111) surface reported in a previous study by Papoian and coworkers.[11] Légaré[38] recently showed that for H atoms on a Pt crystalline surface the desorption energy is strongly coverage-dependent. We therefore expect that both the H_2 dissociative chemisorption energy and H desorption energy on a fully saturated Pt cluster will be considerably higher than the ones on a Pt crystalline surface at a high coverage.

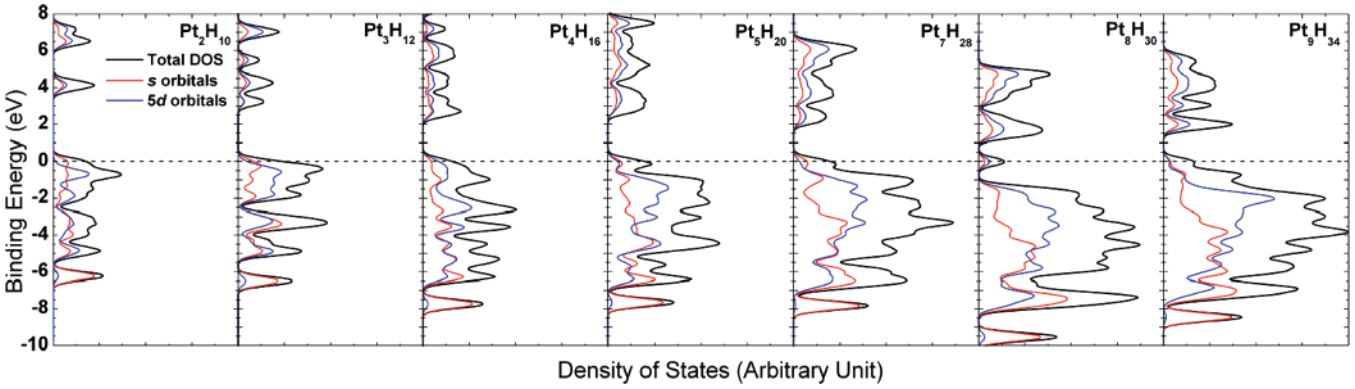

Figure 6. Calculated density of states of Pt clusters saturated with H atoms.

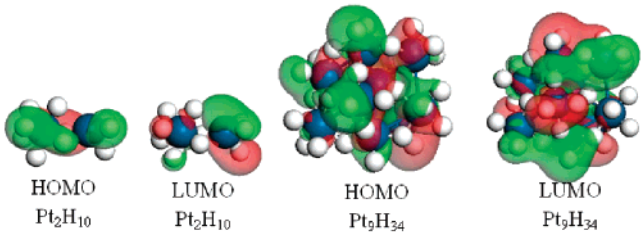

Figure 7. Calculated HOMOs and LUMOs of Pt_2H_{10} and Pt_9H_{34}.

Figure 5 displays the number of H atoms versus size of clusters at full saturation. It shows that the number of H atoms increases almost linearly with the size of clusters. Although we expect such a quasilinear relationship would not hold for much larger clusters, nevertheless, the catalytic efficiency of small clusters for H_2 dissociative chemisorption is still remarkable.

Our previous studies on the magnetism of Pt clusters indicate that most of the bare clusters exhibit magnetic moments due to the unpaired 5d electrons.[28] Upon H_2 dissociative chemisorption, these 5d orbitals interact with the 1s orbital of the H atoms strongly, leading to electron pairing and hydride formation. As a consequence, the electronically open-shell systems become closed-shell systems. Indeed, the calculated results indicate that all unpaired spins are diminished. Figure 6 displays the calculated density of states (DOS) of the fully saturated Pt clusters. For convenience, only the spin-up states are shown since the spin-down species are identical to those of the spin-up's. Detailed analysis indicates that the valence bands are contributed mostly by the 5d orbitals of Pt atoms and the 1s orbital of H atoms. The conduction bands are mostly contributed by the 5d and 6s orbitals of Pt atoms. This is consistent with the calculated charge transfer from Pt clusters to H atoms. In particular, it is interesting to note that the band gaps, ranging from 0.9 to 2.8 eV, are gradually shrinking as the size of clusters increases. This is because for larger clusters, all bridge sites are nearly fully saturated and the symmetric 1s orbital of H atoms readily overlaps with the neighboring 5d orbitals of Pt atoms, resulting in electron delocalization in the entire cluster. Indeed, the calculated highest occupied and lowest unoccupied molecular orbitals (HOMOs and LUMOs) of Pt_2H_{10} and Pt_9H_{34}, shown in Figure 7, indicate strong orbital overlaps in the larger cluster, and orbital overlaps for the smaller cluster are more localized. It is also worth noting that the trend of band gap evolution with cluster size at full saturation is in contrast to the band gap trend for a given cluster with increasing H coverage as was observed for Pt_6 reported previously,[25] where the gradually increased band gaps with H coverage are due to the change from metallic bonding to covalent bonding.

Finally, we note that a recent experiment on an icosahedral Pt_{13} cluster residing in an NaY zeolite, conducted by Liu et al.,[12] reported that the cluster remains paramagnetic upon H_2 dissociative chemisorption. Up to 30 H atoms were found to bind to 12 surface Pt atoms. The H/Pt ratio is smaller than what is reported here, likely due to the fact that the Pt atom at the cluster center is not accessible by H atoms and that the cluster is confined in the zeolitic channel, which prevents the cluster from fully being covered by H atoms. As a consequence, the cluster is unable to form bonds with H atoms to its maximum capacity, resulting in some of the 5d electrons remaining unpaired. Thus the cluster is magnetic. However, all the Pt atoms in the clusters selected in our study are accessible by H atoms. Our calculations suggest that before these clusters reach full H saturation, they also exhibit a certain degree of magnetism, depending on H coverage. Upon full H saturation, all the Pt atoms reach their full capacity to form Pt−H bonds and their 5d electrons become fully paired with vanishing magnetic moments.

4. Summary

Transition metal-catalyzed hydrogenation and dehydrogenation is one of the most important reactions in heterogeneous catalysis, in which the catalysts are dispersed as nanoparticles on supports. Under the typical operating conditions of a catalytic system, a certain pressure of H_2 molecules is usually maintained. A theoretical model capable of adequately describing the catalytic system is of essential importance for understanding of detailed reactive processes. As an alternative to conventional theoretical models using crystalline surfaces to represent catalysts, we instead use small Pt clusters as a model of catalyst to investigate the critical physicochemical properties of Pt catalyst in catalyzing hydrogenation and dehydrogenation reactions upon full hydrogen saturation. Our main emphasis in the present work was on the dissociative chemisorption energy of H_2 molecule and the sequential desorption energy of H atom under full cluster saturation conditions.

Similarly to what was reported for crystalline Pt surfaces, we found that H_2 dissociative chemisorption energies and H desorption energies in small Pt clusters are strongly coverage-dependent. These energies in general decline with H coverage, and at the threshold of saturation, the H_2 chemisorption and H desorption energies each fall within a narrow range that is comparable to the results for a bare Pt(111) surface at zero coverage. The H_2 dissociative chemisorption process is nearly barrierless on the unsaturated clusters, again comparable to results for a bare Pt(111) surface at zero coverage. As the coverage of the crystalline surfaces increases, both the H_2 dissociative chemisorption and H desorption energies are

expected to decrease.[11] The higher activity of the metal clusters, compared with single crystalline surfaces, arises from the fact that clusters possess sharp corners and edges exposed to gas species. It was found that the Pt clusters expand steadily as the H coverage increases. The on-top sites on the clusters are first populated, followed by the edge sites and then the hollow sites, until the clusters are fully saturated. Hirshfeld population analysis indicates that charge transfer from Pt clusters to H atoms increases with H loading, resulting in sequential change of metallic bonds to covalent bonds in the metal hydrides. As the size of clusters increases, the calculated band gaps of the saturated clusters gradually diminish due to the strong orbital overlaps between the 1s orbital of H atoms and 5d orbitals of Pt atoms at the edge sites, leading to electron delocalization in these clusters. Our calculations suggest that the Pt:H ratio is nearly constant at full saturation, except when some of the metal atoms residing at the core of the clusters are not accessible to H atoms.

Although the cluster size selected in the present study is much smaller than the particle size used in realistic heterogeneous catalytic systems, studies at the subnanoscale provide useful insight into the detailed catalytic processes. Some of the properties may not change significantly with the particle size of catalysts. Understanding of these properties is of fundamental importance in design of novel catalysts for a wide variety of applications.

Acknowledgment. This work was supported in part by the Research Foundation for Outstanding Young Teachers, China University of Geosciences, Wuhan, China (Grant CUGQNL0519). We gratefully acknowledge the critical reading of the manuscript by Professor N. Balakrishnan.

References and Notes

(1) Nakatsuji, H.; Matsuzaki, Y.; Yonezawa, T. *J. Chem. Phys.* **1988**, *88*, 5759.
(2) Yang, B.; Lu, Q.; Wang, Y.; Zhuang, L.; Lu, J.; Liu, P.; Wang, J.; Wang, R. *Chem. Mater.* **2003**, *15*, 3552.
(3) Qun, T. Z.; Yan, X. F.; Kang, S. P. *J. Mater. Sci.* **2004**, *V39*, 1507.
(4) Gland, J. L.; Baron, K.; Somorjai, G. A. *J. Catal.* **1975**, *36*, 305.
(5) Godbey, D. J.; Somorjai, G. A. *Surf. Sci.* **1988**, *204*, 301.
(6) Ankudinov, A. L.; Rehr, J. J.; Low, J.; Bare, S. R. *Phys. Rev. Lett.* **2001**, *86*, 1642.
(7) Newuwenhuys, B. E. *Surf. Sci.* **1976**, *59*, 430.
(8) Christmann, K. R.; Palczewska, W. *Hydrogen Effects in Catalysis*; Marcel Dekker: New York, 1988.
(9) Verheij, L. K.; Hugenschmidt, M. B.; Anton, A. B.; Poelsema, B.; Comsa, G. *Surf. Sci.* **1989**, *210*, 1.
(10) Verheij, L. K.; Hugenschmidt, M. B. *Surf. Sci.* **1995**, *324*, 185.
(11) Papoian, G.; Norskov, J. K.; Hoffmann, R. *J. Am. Chem. Soc.* **2000**, *122*, 4129.
(12) Liu, X.; Dilger, H.; Eichel, R. A.; Kunstmann, J.; Roduner, E. *J. Phys. Chem. B* **2006**, *110*, 2013.
(13) Parker, S. F.; Frost, C. D.; Telling, M.; Albers, P.; Lopez, M.; Seitz, K. *Catal. Today* **2006**, *114*, 418.
(14) Vincent, J. K.; Olsen, R. A.; Kroes, G. J.; Baerends, E. J. *Surf. Sci.* **2004**, *573*, 433.
(15) Pijper, E.; Kroes, G. J.; Olsen, R. A.; Baerends, E. J. *J. Chem. Phys.* **2002**, *117*, 5885.
(16) Olsen, R. A.; Kroes, G. J.; Baerends, E. J. *J. Chem. Phys.* **1999**, *111*, 11155.
(17) Dai, D.; Liao, D. W.; Balasubramanian, K. *J. Chem. Phys.* **1995**, *102*, 7530.
(18) Balasubramanian, K. *J. Chem. Phys.* **1991**, *94*, 1253.
(19) Okamoto, Y. *Chem. Phys. Lett.* **2006**, *429*, 209.
(20) Cruz, A.; Bertin, V.; Poulain, E.; Benitez, J. I.; Castillo, S. *J. Chem. Phys.* **2004**, *120*, 6222.
(21) Richter, L. J.; Ho, W. *Phys. Rev. B* **1987**, *36*, 9797.
(22) Gdowski, G. E.; Fair, J. A.; Madix, R. J. *Surf. Sci.* **1983**, *127*, 541.
(23) Au, C. T.; Zhou, T. J.; Lai, W. J. *Catal. Lett.* **1999**, *62*, 147.
(24) Watari, N.; Ohnishi, S. *J. Chem. Phys.* **1997**, *106*, 7531.
(25) Chen, L.; Cooper, A. C.; Pez, G. P.; Cheng, H. *J. Phys. Chem. C* **2007**, *111*, 5514.
(26) Aprà, E.; Fortunelli, A. *J. Phys. Chem. A* **2003**, *107*, 2934.
(27) Watari, N.; Ohnishi, S. *Phys. Rev. B* **1998**, *58*, 1665.
(28) Nie, A.; Wu, J.; Zhou, C.; Yao, S.; Luo, C.; Forrey, R. C.; Cheng, H. *Int. J. Quantum Chem.* **2007**, *107*, 219.
(29) Perdew, J. P.; Chevary, J. A.; Vosko, S. H.; Jackson, K. A.; Pederson, M. R. *Phys. Rev. B* **1992**, *46*, 6671.
(30) Perdew, J. P.; Burke, K.; Ernzerhof, M. *Phys. Rev. Lett.* **1996**, *77*, 3865.
(31) Delley, B. *J. Chem. Phys.* **1990**, *92*, 508.
(32) Delley, B. *J. Phys. Chem.* **1996**, *100*, 6107.
(33) Delley, B. *J. Chem. Phys.* **2000**, *113*, 7756.
(34) Hirshfeld, F. L. *Theor. Chim. Acta B* **1977**, *44*, 129.
(35) Halgren, T. A.; Lipscomb, W. N. *Chem. Phys. Lett.* **1977**, *49*, 225.
(36) Nosé, S. *Mol. Phys.* **1984**, *52*, 255.
(37) Martyna, G. J.; Tuckerman, M. E.; Tobias, M. E. *Mol. Phys.* **1996**, *87*, 1117.
(38) Légaré, P. *Surf. Sci.* **2004**, *559*, 169.